



Published in final edited form as:

*Anal Chem.* 2011 September 1; 83(17): 6883–6889. doi:10.1021/ac201269f.

## Improving Aptamer Selection Efficiency through Volume Dilution, Magnetic Concentration, and Continuous Washing in Microfluidic Channels

Seung Soo Oh<sup>1</sup>, Kareem M. Ahmad<sup>2</sup>, Minseon Cho<sup>1,3</sup>, Seon Kim<sup>4</sup>, Yi Xiao<sup>1,3,\*</sup>, and H. Tom Soh<sup>1,2,3,\*</sup>

<sup>1</sup>Materials Department, University of California, Santa Barbara, CA 93106

<sup>2</sup>Biomolecular Science and Engineering Program, University of California, Santa Barbara, CA 93106

<sup>3</sup>Department of Mechanical Engineering, University of California, Santa Barbara, CA 93106

<sup>4</sup>Department of Electrical and Computer Engineering, University of California, Santa Barbara, CA 93106

### Abstract

The generation of nucleic acid aptamers with high affinity typically entails a time-consuming, iterative process of binding, separation, and amplification. It would therefore be beneficial to develop an efficient selection strategy that can generate these high quality aptamers rapidly, economically, and reproducibly. Toward this goal, we have developed a method that efficiently generates DNA aptamers with slow off-rates. This methodology, called VDC-MSELEX, pairs the volume dilution challenge process with microfluidic separation for magnetic bead-assisted aptamer selection. This method offers improved aptamer selection efficiencies through the application of highly stringent selection conditions: it retrieves a small number ( $< 10^6$ ) of magnetic beads suspended in a large volume ( $> 50$  mL) and concentrates them into a microfluidic chamber (8  $\mu$ L) with minimal loss for continuous washing. We performed three rounds of the VDC-MSELEX using streptavidin (SA) as the target, and obtained new DNA aptamer sequences with low nanomolar affinity that specifically bind to the SA proteins.

Aptamers are a class of synthetic, nucleic acid-based affinity reagents that are capable of specifically binding to a range of targets including small molecules,<sup>1</sup> proteins,<sup>2</sup> viruses,<sup>3</sup> and whole cells.<sup>4-5</sup> Aptamers offer many useful characteristics; they are chemically synthesized, thermo-stable, readily modified, and can be further engineered to perform complex functions upon binding.<sup>6-7</sup> Aptamers are typically generated from random nucleic acid libraries through multiple cycles of SELEX (systematic evolution of ligands by exponential enrichment)—an iterative process of binding, separation and amplification.<sup>8-9</sup> This procedure requires significant time and labor, and the resulting binding affinity and specificity critically depend on the selection process. Thus, there is a need for an efficient selection method that can rapidly and reproducibly generate high quality aptamers with minimal resources. We have previously described the advantages of using microfluidics technology for aptamer selection (M-SELEX), which include the capability to apply high-stringency selection conditions by using small quantities of target molecule, and the ability to control fluid flow-rate within the microchannel in order to efficiently remove weakly- or

\*Corresponding authors: yixiao@physics.ucsb.edu and tsoh@enr.ucsb.edu.

non-specifically-bound nucleic acids with minimal target loss. These features have yielded high affinity molecules within fewer rounds of selection.<sup>10–13</sup>

In this work, we exploit the microfluidic capability to concentrate a small number of magnetic beads suspended in a large volume into a miniaturized chamber and explore the effect of sample volume dilution, an important selection parameter that controls the off-rates of aptamers ( $k_{\text{off}}$ ). Previously, Gold and co-workers described the sample volume dilution challenge technique,<sup>14</sup> wherein aptamer-target complexes are subjected to re-equilibration in increasing buffer volumes during selection. This technique yielded aptamers with better off-rates and lower equilibrium dissociation constants ( $K_d = k_{\text{off}}/k_{\text{on}}$ ), presumably due to the more efficient dissociation of weakly-bound nucleic acids. In this work, we have integrated volume dilution challenge with the microfluidic selection process (VDC-MSELEX) and demonstrate the selection of aptamers with improved off-rates. Importantly, we have utilized the MicroMagnetic Separation (MMS) device previously developed in our laboratory,<sup>10, 12–13, 15</sup> which offers an excellent platform for volume dilution challenge; we demonstrate the ability to recover a small number of magnetic beads ( $< 10^6$  beads) suspended in a large volume (*e.g.*  $> 50$  mL), and rapidly concentrate them into an 8  $\mu\text{L}$  capture chamber with  $\sim 96\%$  bead recovery within 15 minutes. Furthermore, the MMS chip offers an additional means for removing weakly-bound nucleic acids through high-stringency, continuous washing within the capture chamber. We performed three rounds of VDC-MSELEX using streptavidin (SA) as the target, and observed a significant increase in aptamer selection efficiency, and obtained novel DNA aptamers that specifically bind SA with low nanomolar affinity.

## EXPERIMENTAL SECTION

### Reagents

Streptavidin was purchased from Roche Applied Science (Penzberg, Germany). Human  $\alpha$ -thrombin was purchased from Hematologic Technologies Inc. (Essex Junction, VT). Bovine serum albumin (BSA), N-hydroxy-succinimide (NHS) and 1-ethyl-3-(3-dimethylaminopropyl) carbodiimide hydrochloride (EDC) were purchased from Sigma-Aldrich (Saint Louis, MO) and used without further purification. Agarose was purchased from Fisher Scientific (Pittsburgh, PA). GoTaq Hot Start Colorless Master Mix and PCR water were purchased from Promega (Madison, WI). Dynabeads MyOne C1 SA-coated beads and M-270 carboxylic acid-coated beads were purchased from Invitrogen (Carlsbad, CA). Lambda exonuclease enzyme (5000 U/mL) and 10 $\times$  lambda exonuclease reaction buffer were purchased from New England BioLabs (Ipswich, MA). The random DNA library was synthesized with hand-mixing by Integrated DNA Technologies (Coralville, IA) and purified via PAGE. Each single-stranded DNA (ssDNA) library component consists of a central 60-mer random region flanked by two 20-mer PCR primer sequences. Unlabeled, phosphorylated and FAM-labeled PCR primers (see Supporting Information, Table S1) were synthesized by Biosearch Technologies (Novato, CA) and purified via HPLC. The binding and washing buffer used for SA aptamer selection consisted of 20 mM Tris, pH 7.6, 150 mM NaCl, 2 mM MgCl<sub>2</sub>, and 0.02% Tween20 (v/v).

### Library Amplification

We performed PCR amplification with a 100  $\mu\text{L}$  reaction mixture containing 50  $\mu\text{L}$  of GoTaq Hot Start Master Mix, 4  $\mu\text{L}$  of 100  $\mu\text{M}$  forward primer, 4  $\mu\text{L}$  of 100  $\mu\text{M}$  phosphorylated reverse primer, 4  $\mu\text{L}$  of 1  $\mu\text{M}$  random ssDNA stock and 38  $\mu\text{L}$  of nuclease-free water. The PCR program consisted of 5 cycles at 95  $^\circ\text{C}$  for 5 min, 51  $^\circ\text{C}$  for 1 min and 72  $^\circ\text{C}$  for 20 min, followed by an additional 4 cycles of 95  $^\circ\text{C}$  for 30 sec, 58  $^\circ\text{C}$  for 1 min and 72  $^\circ\text{C}$  for 1 min, and finally a 14-min extension at 72  $^\circ\text{C}$ . PCR products were

concentrated by ethanol precipitation and resolved on a 2% agarose gel. 100-base pair double-stranded DNAs (dsDNAs) were extracted and purified using a QIAquick gel extraction kit (Qiagen, Venlo, Netherlands) following the manufacturer's protocol. Purified dsDNAs were subsequently digested with lambda exonuclease using the method described below, and the resulting ssDNA pool was further purified by phenol/chloroform extraction and ethanol precipitation. The total PCR reaction volume was adjusted to yield 1 nmole of amplified ssDNA pool.

### PCR Amplification

We performed a pilot PCR to optimize the number of cycles for amplifying the eluted sample during selection. A PCR mixture containing 50  $\mu\text{L}$  of GoTaq Hot Start Master Mix, 0.25  $\mu\text{L}$  of 100  $\mu\text{M}$  forward primer, 0.25  $\mu\text{L}$  of 100  $\mu\text{M}$  phosphorylated reverse primer and 39.5  $\mu\text{L}$  of nuclease-free water was prepared, and then combined with 10  $\mu\text{L}$  of the eluted beads from the MMS chip for a final volume of 100  $\mu\text{L}$ . GoTaq Hot Start polymerase was activated prior to PCR by heating the reaction mixture to 95  $^{\circ}\text{C}$  for 2 min, followed by 20 cycles of a rapid three-step PCR (30 sec at 95  $^{\circ}\text{C}$ , 30 sec at 56  $^{\circ}\text{C}$ , 30 sec at 72  $^{\circ}\text{C}$ ). During the extension step of each cycle, 6  $\mu\text{L}$  of PCR mixture were collected and resolved on a 10% PAGE-TBE (1 $\times$  TBE: 89 mM Tris borate, 2 mM  $\text{Na}_2\text{EDTA}$ , pH 8.3) gel to determine the optimal PCR amplification cycle number with minimal by-products. The collected aptamer pools from each round were PCR amplified at this optimized cycle number.

### Characterization of Washing Efficiency

0.5  $\mu\text{L}$  of MyOne C1 SA-beads were incubated with 50 pmol of ssDNA library in 50  $\mu\text{L}$  of SA binding buffer for 2 hours followed by a 30-min wash using one of three different methods: MMS chip washing, volume dilution challenge and combined washing. For continuous washing in the MMS chip, the flow rate was 50 mL/hr, and for the dilution challenge the volume was diluted 100-fold. The combined method consisted of a 25-min dilution challenge and 5-min additional MMS chip washing. After washing, beads were eluted into 600  $\mu\text{L}$  of fresh buffer. To compare washing efficiencies, real-time PCR (RT-PCR) was performed, and the amounts of ssDNA bound to SA were determined by monitoring threshold cycles ( $C_T$ ). The reaction solutions were prepared with 10  $\mu\text{L}$  iQ SYBR Green Supermix (Bio-Rad Laboratories, Hercules, CA), 8.8  $\mu\text{L}$  PCR water, 0.1  $\mu\text{L}$  each of 0.1 mM forward and reverse primer and 1  $\mu\text{L}$  eluted bead solution.  $C_T$  values for each washing method were monitored using the iQ<sup>5</sup> RT-PCR Detection System (Bio-Rad Laboratories).

### ssDNA Generation

Purified dsDNA solution was mixed with a specific volume of lambda exonuclease enzyme (*e.g.*, 1  $\mu\text{g}$  of dsDNA with 1  $\mu\text{L}$  of lambda exonuclease stock), and the mixture was adjusted to yield 1 $\times$  lambda exonuclease reaction buffer conditions using 10 $\times$  concentrated buffer stock. This mixture was immediately incubated at 37  $^{\circ}\text{C}$  for 2 hrs followed by an additional 10-min incubation at 75  $^{\circ}\text{C}$  to stop the enzymatic reaction. After digestion, ssDNA was purified with phenol/chloroform extraction and ethanol precipitation and completely dried out before use.

### Affinity and Specificity Measurements

The average dissociation constant of each ssDNA pool was measured via a fluorescence binding assay. FAM-labeled ssDNA pools were diluted to several different concentrations (from 0 to 100 nM) in 140  $\mu\text{L}$  of binding buffer; these dilutions were heated at 95  $^{\circ}\text{C}$  for 10 min, immediately cooled on ice for 10 min and then incubated for another 10 min at room temperature (RT). Subsequently, these various heat-treated ssDNA solutions were incubated

with target-coated beads at RT for 1 hour in a total volume of 150  $\mu\text{L}$ . We measured the  $K_d$  for pools from each round, including the amplified library, using 0.1  $\mu\text{L}$  of Dynabeads MyOne C1 SA-coated beads ( $7 \times 10^9$  beads/mL,  $3.01 \times 10^5$  SA molecules/bead, 1.0  $\mu\text{m}$  in diameter). The specificity of the synthesized aptamer sequences was tested with M-270 carboxylic acid-coated beads ( $2 \times 10^9$  beads/mL, 2.8  $\mu\text{m}$  in diameter) because these beads yielded closer matching of surface densities of SA, BSA and thrombin. The molecules were immobilized on the beads through the EDC-NHS coupling process using the manufacturer's protocol, and quantified with the NanoOrange Protein Quantitation Kit (Invitrogen). We used 0.3  $\mu\text{L}$  of SA ( $3.42 \times 10^5$  molecules/bead), 0.4  $\mu\text{L}$  of BSA ( $2.66 \times 10^5$  molecules/bead), and 0.3  $\mu\text{L}$  of thrombin ( $3.22 \times 10^5$  molecules/bead) and 0.3  $\mu\text{L}$  of tris coated beads. After incubating the ssDNA solutions with target-coated beads, the magnetic beads were washed three times with binding buffer and magnetic separation was used to eliminate unbound ssDNAs. Bound ssDNAs were then released into 55  $\mu\text{L}$  of binding buffer by heating the aptamer-bound beads at 95  $^\circ\text{C}$  for 10 min while shaking (300 rpm). Next, 50  $\mu\text{L}$  of each eluate was transferred to a black 96-well microplate (Microfluor 2, Thermo Scientific, Waltham, MA), and the amount of released ssDNA was determined by fluorescence measurement using a microplate reader (Tecan, San Jose, CA). Finally, dissociation constants ( $K_d$ ) were calculated from the calibrated curve fitting using the equation  $Y = B_{\text{max}} \times X / (K_d + X)$  where X is the concentration of the ssDNA and  $B_{\text{max}}$  is the fluorescence value at saturation.

### Cloning and Sequencing of Selected Aptamers

PCR products were amplified with unlabeled primers at the optimized cycle number, purified using the MiniElute PCR Purification Kit (Qiagen) with the manufacturer's protocol and cloned into *Escherichia coli* using the TOPO TA Cloning Kit (Invitrogen). 20 colonies each from rounds 2–3 were randomly picked and sequenced at Genewiz Inc. (South Plainfield, NJ). The sequences were then analyzed and aligned using Geneious v5.1 (Biomatters Ltd., New Zealand). Two representative aptamer sequences from each round were amplified with phosphorylated reverse primers and FAM-labeled forward primers for further fluorescence affinity measurements.

### Relative Binding Affinity Assay

A PCR mixture containing 10  $\mu\text{L}$  of GoTaq Hot Start Master Mix, 0.2  $\mu\text{L}$  of 100  $\mu\text{M}$  forward primer, 0.2  $\mu\text{L}$  of 100  $\mu\text{M}$  reverse primer and 9.6  $\mu\text{L}$  of nuclease-free water was prepared, and a small amount of each sequenced colony-derived DNA sample was transferred into 20  $\mu\text{L}$  of PCR mixture. Prepared PCR mixtures were amplified as described above for 25 cycles. PCR products were diluted 100-fold with nuclease-free water, and a small quantity of the diluted solution was further amplified for 8 cycles based on the procedure described above, after which FAM-labeled ssDNA pools were generated for each sample via lambda digestion and purified. 150  $\mu\text{L}$  of 50 nM FAM-labeled ssDNA solution from each colony was prepared in SA binding buffer. The remaining steps of binding measurement were performed as described above.

## RESULTS AND DISCUSSION

### Overview of Microfluidic Selection Process

The VDC-MSELEX process (Fig. 1) begins with the preparation of the random DNA library. The initial ssDNA library ( $\sim 100$  pmol total) contains oligos with a 60-base random region flanked by two 20-base primer regions. We PCR amplified the library with phosphorylated reverse primer, after which we selectively digested the phosphorylated strands from the dsDNA amplicons with lambda exonuclease<sup>16–17</sup> to obtain ssDNA (Fig. 1A). Compared to other ssDNA generation methods (e.g., asymmetric PCR and streptavidin

affinity purification), we have found that lambda exonuclease digestion generates ssDNA with higher purity and efficiency, presumably because the process produces less background contamination than other methods (*e.g.*, dsDNA templates, biotinylated complementary strands, SA molecules, etc.).<sup>18</sup>

The amplified ssDNA library, containing approximately  $6 \times 10^{14}$  molecules and  $\sim 10$  copies of each individual sequence, was incubated with SA-coated magnetic beads in 50  $\mu$ l binding buffer for 1 hr (Fig. 1B). After incubation, we immediately performed the volume dilution challenge by diluting the sample into larger volumes of fresh binding buffer (round 1 = 1 mL, round 2 = 10 mL, round 3 = 50 mL, representing dilution factors of 20, 200 and 1000, respectively) to dissociate ssDNAs with high  $k_{\text{off}}$  (Fig. 1C). We then pumped the diluted samples into the MMS chip to retrieve the magnetic beads and separate target-bound aptamers from unbound oligos (Fig. 1D). During the bead retrieval step, we used high buffer flow-rates (50 ml/hr for rounds 1 & 2 and 100 ml/hr for round 3, representing average fluid velocity of  $\sim 5$  cm/s and  $\sim 10$  cm/s, respectively) to continuously remove weakly- and non-specifically-bound oligos from the device. After the separation, we removed the external magnets, and eluted the magnetic beads carrying target-bound aptamers from the device (Fig. 1E). We note that the bead recovery with the MMS device was excellent: 96% of the initial pool of  $10^6$  beads were successfully recovered after sample volume dilution, MMS trapping and high flow-rate continuous washing.

Next, we PCR amplified the enriched aptamers with phosphorylated reverse primers and unmodified forward primers (Fig. 1F). We optimized the PCR cycle number for each selection cycle with a pilot PCR process<sup>19</sup> to eliminate undesirable byproducts. We then generated ssDNA by digesting phosphorylated reverse strands of the amplified PCR product with lambda exonuclease (Fig. 1G). After digestion, we purified the resulting ssDNA pool by phenol/chloroform extraction and ethanol precipitation (Fig. 1H), and the concentration of ssDNA was measured via UV-vis absorption. Each round of selection after PCR amplification and ssDNA generation yielded slightly more than 100 pmol, and we used the majority of the pool ( $\sim 100$  pmol) for the next round of selection.

### Comparison of Washing Methods

To quantitatively compare the efficiencies of different washing strategies, we used real-time PCR (RT-PCR) to measure the amount of remaining DNA after washing with VDC, continuous washing or a combination of the two. Specifically, we applied 30 minutes of washing with each method and measured the amount of bead-bound ssDNA with RT-PCR. We used  $\Delta C_T$  (difference in threshold cycle value between the sample and a negative control with no template DNA) to quantify differences in template copy number in samples obtained from the three methods.<sup>20</sup> We found that VDC paired with continuous washing offers the most effective means of removing weakly- or non-specifically-bound nucleic acids. For example, this combined approach yielded  $\sim 30$ -fold and  $\sim 10$ -fold less DNA than samples obtained with continuous washing only or VDC only, respectively (Fig S1). We note that, during the washing, we often observe the formation of clusters due to mutual magnetization among the beads within the MMS chip. This phenomenon may cause some of the bead surfaces, specifically those in the interior of the clusters, to be inaccessible by the wash buffer – even when a large volume of high velocity, continuous washing is employed. On the other hand, VDC allows uninhibited access to bead surfaces, however, it does not provide stringent washing. We thus believe that the combination of VDC and continuous washing allows the most effective washing strategy to remove the ssDNA as measured by the quantitative PCR results.



## Comparison of Selection Efficiencies

We performed three rounds of VDC-MSELEX and measured the bulk affinity of each enriched pool for SA with a bead-based fluorescence assay.<sup>13, 21</sup> In order to perform affinity measurements, we PCR amplified the initial random library and enriched pools using phosphorylated reverse primers and FAM-labeled forward primers. Next, FAM-modified ssDNA pools were generated by lambda digestion and purified. As expected, the initial random library exhibited negligible binding affinity to the SA target (Fig. 2, star). The first round (R1) and second round (R2) pools showed a slight but measurable increase in affinity to the target (Fig. 2, triangle and circle, respectively), but the third round pool (R3) showed a significant increase, with a bulk dissociation constant ( $K_d$ ) of  $62.5 \pm 5.1$  nM (Fig. 2, square).

In order to calibrate the selection efficiency of VDC-MSELEX, we performed two additional selections via conventional magnetic separation and the MMS chip (without volume dilution). For the conventional magnetic selection, we used the Magnetic Particle Concentrator (MPC, Invitrogen), and manually performed the buffer exchange with 1 mL of fresh buffer every 5 min for the washing step. We performed three rounds of selections for each method under the same experimental conditions as those used in the VDC-MSELEX including target concentration and the washing time. Compared to the bulk affinity of the final pool obtained with the VDC-MSELEX method, the affinities obtained with MPC (Fig S3, triangle) and MMS without volume dilution (Fig S3, circle) were significantly lower. These results clearly demonstrate that the VDC-MSELEX method offers significantly higher selection efficiencies.

## Affinity and Specificity of the Selected Sequences

To characterize individual aptamer sequences from the enriched pools using the VDC-MSELEX, we cloned the R2 and R3 pools into *E. coli* and randomly picked and sequenced 20 colonies from each pool. All 20 sequences cloned from the R2 pool were distinct from each other and showed no consensus groups (Fig S2). In contrast, sequences obtained from the R3 pool revealed a dominant consensus group that constituted 40% of the total population (Fig. 3A). The similarity of the sequences was remarkably high; we observed that the sequences of clone 5 and clone 17 differ by only a single nucleotide. Likewise, the only sequence difference between clone 6 and the consensus group is a single base deletion. The other 12 orphan sequences (clones 2, 3, 4, 8, 10, 13, 14, 15, 16, 18, 19, 20) did not show any obvious consensus. In order to rapidly identify the sequences with highest affinities, we synthesized the cloned sequences from R3 with FAM labels, measured their relative binding affinity to SA and rank-ordered the clones based on fluorescence signal amplitude (Fig 3B). Briefly, 150  $\mu$ L of 50 nM FAM-labeled sequences were incubated with 0.1  $\mu$ L of SA-coated beads ( $10^7$  beads) in binding buffer for 1 hour. After washing the beads with fresh buffer, the bound aptamers were eluted by heating and relative amounts were measured via fluorescence. We found that the consensus sequences gave the highest fluorescence intensity, while orphan sequences produced minimal fluorescence signal that was similar to the fluorescence amplitude of the starting library.

We investigated whether the single nucleotide substitution (T/C) at the 74<sup>th</sup> base of the consensus sequence results in any differences in SA affinity or specificity. To do so, we synthesized these two sequences with FAM labels and measured their  $K_d$  values (Fig. 4, left column). In order to use similar surface density of SA and other proteins for the specificity measurement, we used the well-established EDC/NHS chemistry to immobilize the proteins on Dynal M-270 beads. We found that both sequences – SAAT (SA Aptamer with T74) and SAAC (with C74) – showed similar  $K_d$  values, where  $K_d$  (SAAT) =  $36.2 \pm 3.6$  nM and  $K_d$  (SAAC) =  $35.2 \pm 2.4$  nM. However, the two sequences showed notable differences in their specificity based on binding to unrelated molecules bovine serum albumin (BSA), Human  $\alpha$ -

thrombin and Tris (Fig. 4, left column, inset). Both sequences showed low affinities to BSA, thrombin and Tris; however, in comparison to SAAT, the SAAC sequence showed ~2-fold lower binding to BSA and thrombin, and ~3-fold lower binding to Tris-coated beads (Fig. 4). Our observation, that a single nucleotide difference can significantly affect the affinity and the specificity of an aptamer, has been previously reported for other targets.<sup>22–23</sup>

To understand the structural differences between the aptamers, we modeled the SAAC and SAAT sequences using the *mfold* software (Fig. 4, right column).<sup>24</sup> We found that both sequences contained significant secondary structure, including protruding loops and stems. From the Gibbs free energy calculations, the SAAC structure (−6.42 kcal/mol) appears to be more stable than the SAAT structure (−5.84 kcal/mol). Interestingly, we found the CGC, GCG and GC motifs displayed in the bulge and hairpin regions of the SAAC aptamer to be similar to those found in previously published streptavidin aptamers.<sup>21, 25–27</sup>

## CONCLUSION

In this work, we report an improved method for aptamer selection that combines the advantages of the volume dilution challenge with microfluidics technology. We found that this integration is especially well-matched with our MMS chip, which offers the critical capability to concentrate a small number of magnetic beads ( $< 10^6$  beads) suspended in a large volume (*e.g.*  $> 50$  mL) into an 8  $\mu$ L chamber with ~96% bead recovery within 15 minutes. Once the beads are magnetically captured in the chip, high-stringency, continuous washing can be performed in the device without loss of target to obtain aptamers with low  $k_{\text{off}}$ . Importantly, these features translate to generation of higher affinity aptamers with fewer selection rounds; for example, Stoltenburg *et al.* selected DNA aptamers for streptavidin in 13 rounds using a conventional magnetic column, obtaining molecules with  $K_d$  values of ~56–86 nM. In contrast, we have isolated DNA aptamers with  $K_d$  of  $35.2 \pm 2.4$  nM within 3 rounds. Although immobilization to bead surfaces can pose limitations for some classes of targets (*e.g.* small molecules, cells and tissue surface),<sup>18</sup> a wide variety of conjugation chemistries are available for proteins and other biomolecules. We thus believe that our VDC-MSELEX technique may be useful for a range of targets, as well as different classes of molecular libraries beyond DNA aptamers.

## Supplementary Material

Refer to Web version on PubMed Central for supplementary material.

## Acknowledgments

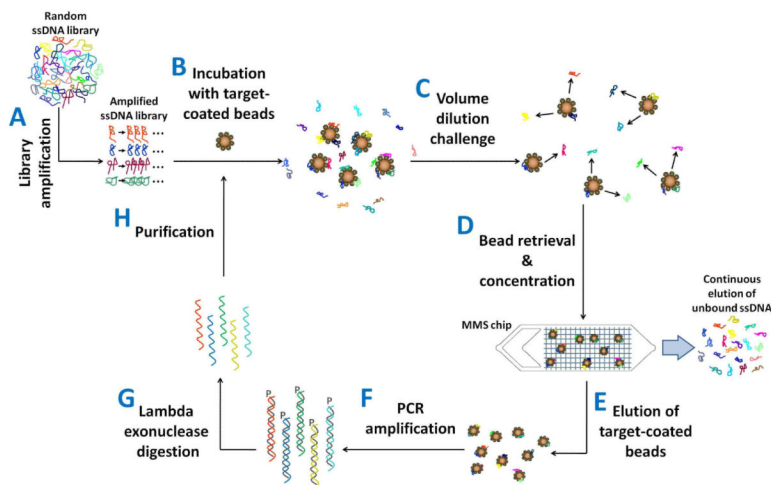
We thank A. Csordas and Q. Gong for the help with library amplification and J.P Wang for the help with the lambda exonuclease digestion method. We are grateful for financial support from the Institute of Collaborative Biotechnologies (ICB) through the Army Research Office, and the National Institutes of Health, Armed Forces Institute for Regenerative Medicine (AFIRM), California Institute for Regenerative Medicine (CIRM) and the Otis Williams Foundation.

## REFERENCES

- (1). Huizenga DE, Szostak JW. *Biochemistry*. 1995; 34:656–665. [PubMed: 7819261]
- (2). Bock LC, Griffin LC, Latham JA, Vermaas EH, Toole JJ. *Nature*. 1992; 355:564–566. [PubMed: 1741036]
- (3). Gopinath SCB, Misono TS, Kawasaki K, Mizuno T, Imai M, Odagiri T, Kumar PKR. *J. Gen. Virol.* 2006; 87:479–487. [PubMed: 16476969]
- (4). Daniels DA, Chen H, Hicke BJ, Swiderek KM, Gold L. *Proc. Natl. Acad. Sci. U.S.A.* 2003; 100:15416–15421. [PubMed: 14676325]

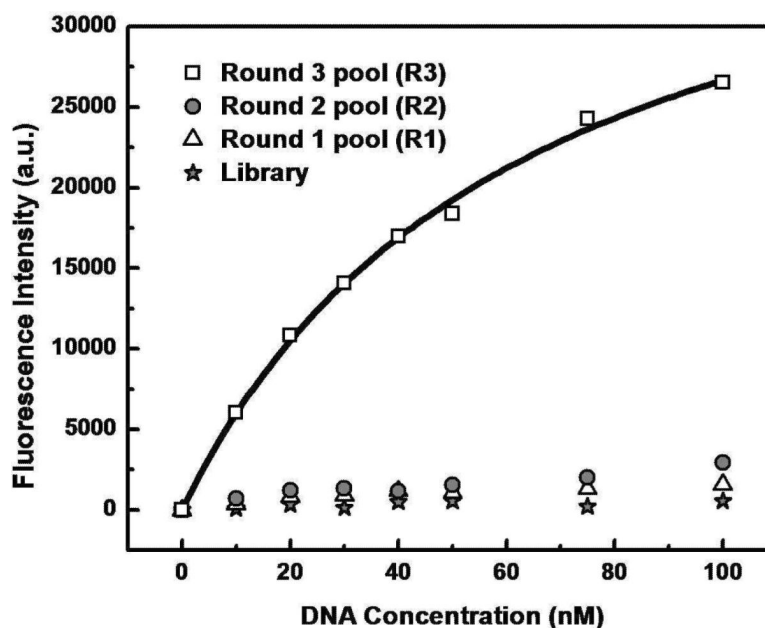
- (5). Shangguan D, Li Y, Tang ZW, Cao ZHC, Chen HW, Mallikaratchy P, Sefah K, Yang CYJ, Tan WH. *Proc. Natl. Acad. Sci. U.S.A.* 2006; 103:11838–11843. [PubMed: 16873550]
- (6). Nutiu R, Li Y. *Angew. Chem. Int. Edit.* 2005; 44:1061–1065.
- (7). Oh SS, Plakos K, Lou X, Xiao Y, Soh HT. *Proc. Natl. Acad. Sci. U.S.A.* 2010; 107:14053–14058. [PubMed: 20660786]
- (8). Ellington AD, Szostak JW. *Nature.* 1990; 346:818–822. [PubMed: 1697402]
- (9). Tuerk C, Gold L. *Science.* 1990; 249:505–510. [PubMed: 2200121]
- (10). Liu Y, Adams JD, Turner K, Cochran FV, Gambhir SS, Soh HT. *Lab Chip.* 2009; 9:1033–1036. [PubMed: 19350081]
- (11). Lou XH, Qian JR, Xiao Y, Viel L, Gerdon AE, Lagally ET, Atzberger P, Tarasow TM, Heeger AJ, Soh HT. *Proc. Natl. Acad. Sci. U.S.A.* 2009; 106:2989–2994. [PubMed: 19202068]
- (12). Qian JR, Lou XH, Zhang YT, Xiao Y, Soh HT. *Anal. Chem.* 2009; 81:5490–5495. [PubMed: 19480397]
- (13). Cho M, Xiao Y, Nie J, Stewart R, Csordas AT, Oh SS, Thomson JA, Soh HT. *Proc. Natl. Acad. Sci. U.S.A.* 2010; 107:15373–15378. [PubMed: 20705898]
- (14). Gold L, Ayers D, Bertino J, Bock C, Bock A, Brody EN, Carter J, Dalby AB, Eaton BE, Fitzwater T, Flather D, Forbes A, Foreman T, Fowler C, Gawande B, Goss M, Gunn M, Gupta S, Halladay D, Heil J, Heilig J, Hicke B, Husar G, Janjic N, Jarvis T, Jennings S, Katilius E, Keeney TR, Kim N, Koch TH, Kraemer S, Kroiss L, Le N, Levine D, Lindsey W, Lollo B, Mayfield W, Mehan M, Mehler R, Nelson SK, Nelson M, Nieuwlandt D, Nikrad M, Ochsner U, Ostroff RM, Otis M, Parker T, Pietrasiewicz S, Resnicow DI, Rohloff J, Sanders G, Sattin S, Schneider D, Singer B, Stanton M, Sterkel A, Stewart A, Stratford S, Vaught JD, Vrkljan M, Walker JJ, Watrobka M, Waugh S, Weiss A, Wilcox SK, Wolfson A, Wolk SK, Zhang C, Zichi D. *PLoS One.* 2010; 5:e15004. [PubMed: 21165148]
- (15). Csordas A, Gerdon AE, Adams JD, Qian J, Oh SS, Xiao Y, Soh HT. *Angew. Chem. Int. Edit.* 2010; 49:355–358.
- (16). Avci-Adali M, Paul A, Wilhelm N, Ziemer G, Wendel HP. *Molecules.* 2010; 15:1–11. [PubMed: 20110867]
- (17). Ruff KM, Snyder TM, Liu DR. *J. Am. Chem. Soc.* 2010; 132:9453–9464. [PubMed: 20565094]
- (18). Paul A, Avci-Adali M, Ziemer G, Wendel HP. *Oligonucleotides.* 2009; 19:243–254. [PubMed: 19732022]
- (19). Tok JB, Fischer NO. *Chem. Commun.* 2008:1883–1885.
- (20). Heid CA, Stevens J, Livak KJ, Williams PM. *Genome Res.* 1996; 6:986–994. [PubMed: 8908518]
- (21). Stoltenburg R, Reinemann C, Strehlitz B. *Anal. Bioanal. Chem.* 2005; 383:83–91. [PubMed: 16052344]
- (22). Luchansky SJ, Nolan SJ, Baranger AM. *J. Am. Chem. Soc.* 2000; 122:7130–7131.
- (23). Katilius E, Flores C, Woodbury NW. *Nucleic Acids Res.* 2007; 35:7626–7635. [PubMed: 17981839]
- (24). Zuker M. *Nucleic Acids Res.* 2003; 31:3406–3415. [PubMed: 12824337]
- (25). Bittker JA, Le BV, Liu DR. *Nat. Biotechnol.* 2002; 20:1024–1029. [PubMed: 12219078]
- (26). Wang C, Yang G, Luo Z, Ding H. *Acta Biochim. Biophys. Sin.* 2009; 41:335–340. [PubMed: 19352549]
- (27). Bing T, Yang X, Mei H, Cao Z, Shangguan D. *Bioorg. Med. Chem.* 2010; 18:1798–1805. [PubMed: 20153201]



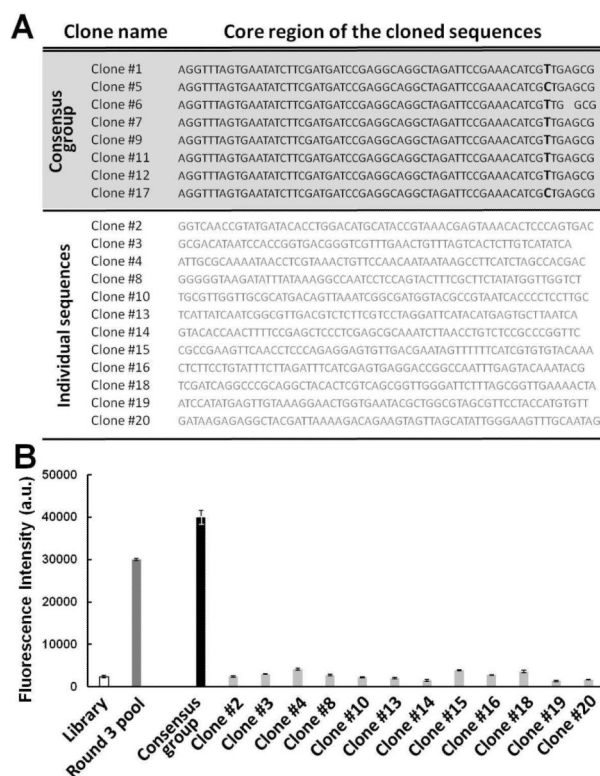


**Figure 1.**

Overview of the VDC-MSELEX selection process. (A) ssDNA library preparation by PCR amplification. The starting ssDNA library consists of  $\sim 10^{14}$  molecules with  $\sim 10$  copies of each individual sequence. (B) Incubation of the target (streptavidin, SA) coated beads with heat-treated ssDNA library in binding buffer. (C) Volume dilution challenge (VDC) to remove aptamers with high  $k_{\text{off}}$ . (D) Continuous elution of unbound ssDNA, magnetic concentration and continuous washing of the beads in the MicroMagnetic Separation (MMS) device. (E) Elution of magnetic beads carrying the target-bound aptamers. (F) PCR amplification of selected aptamers with phosphorylated reverse primers (G) Generation of ssDNA via lambda exonuclease digestion of phosphorylated reverse strands. (H) Purification of digested ssDNA pool by phenol/chloroform extraction and ethanol precipitation.



**Figure 2.** Fluorescence measurements to determine the equilibrium dissociation constants ( $K_d$ ) of enriched pools. The initial library (star) exhibited negligible binding affinity to the target. The enriched pool from first (R1, triangle) and second round (R2, circle) exhibited a slight increase in binding. The third round pool (R3, square) shows dramatically increased affinity with an average  $K_d$  of  $62.5 \pm 5.1$  nM.

**Figure 3.**

(A) 20 cloned sequences from the R3 pool (without flanking primer sites). Sequence alignment revealed one consensus group (8 out of 20 sequences) and 12 orphan sequences. The degree of sequence similarity was extremely high within the consensus group. Two sequences contained a single T/C substitution (clones 5 & 17) and one sequence exhibited a single base deletion (clone 6). The orphan sequences did not exhibit any obvious consensus. (B) Relative binding affinity assay to identify SA-specific aptamer sequences. Only clones from the consensus group (black) exhibited fluorescence intensity greater than R3 (dark grey), compared to the initial library (white) and unconverged cloned sequences (light grey).

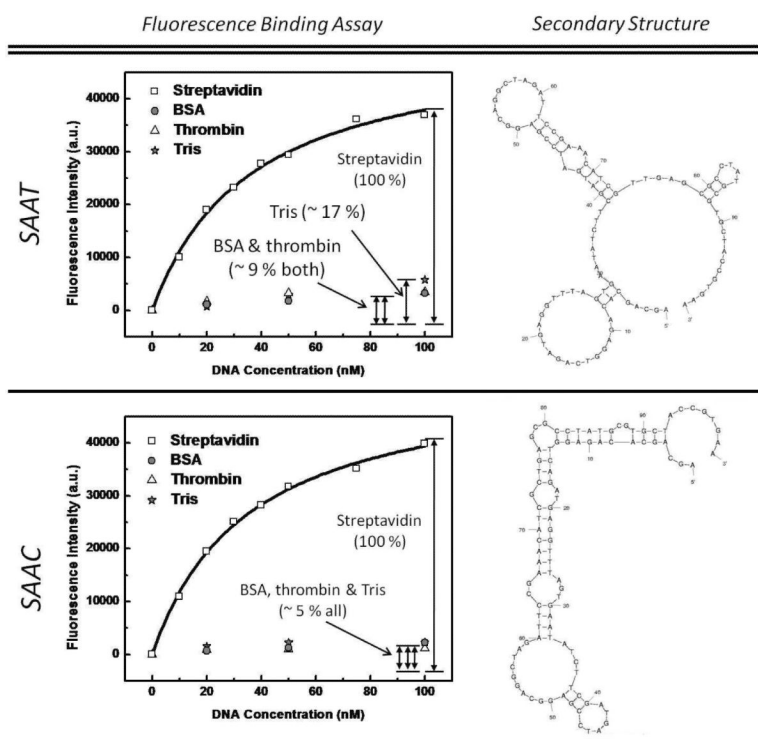


**Figure 4.** Characterization of SA aptamer sequences differing by a single nucleotide. The two consensus sequences showed similar affinities:  $K_d_{SAAC} = 35.2 \pm 2.4$  nM and  $K_d_{SAAT} = 36.2 \pm 3.6$  nM. However, the two sequences have distinct secondary structures and exhibit notable differences in specificity for BSA, thrombin and Tris. In comparison to the SAAT sequence, the SAAC sequence showed ~ 2-fold lower binding to BSA and thrombin, and ~ 3-fold lower binding to Tris coated beads.